

MODELING OF HIGH POWER ICRF HEATING EXPERIMENTS ON TFTR*

C.K. Phillips, J.R. Wilson, M. Bell, E. Fredrickson, J.C. Hosea, A. Khudaleev#,
 R. Majeski, M. Murakami†, M.P. Petrov#, A. Ramsey, J.H. Rogers, G.
 Schilling, C. Skinner, J.E. Stevens, G. Taylor, K.-L. Wong,
 and the TFTR Group
 Princeton Plasma Physics Laboratory, Princeton, NJ 08540

INTRODUCTION

Over the past two years, ICRF heating experiments have been performed on TFTR in the hydrogen minority heating regime with power levels reaching 11.2 MW in helium-4 majority plasmas and 8.4 MW in deuterium majority plasmas¹. For these power levels, the minority hydrogen ions, which comprise typically less than 10% of the total electron density, evolve into a very energetic, anisotropic non-Maxwellian distribution. Indeed, the excess perpendicular stored energy in these plasmas associated with the energetic minority tail ions is often as high as 25% of the total stored energy, as inferred from magnetic measurements. Enhanced losses of 0.5 MeV protons consistent with the presence of an energetic hydrogen component have also been observed². In ICRF heating experiments on JET at comparable and higher power levels and with similar parameters, it has been suggested^{3,4} that finite banana width effects have a noticeable effect on the ICRF power deposition. In particular, models indicate that finite orbit width effects lead to a reduction in the total stored energy and of the tail energy in the center of the plasma, relative to that predicted by the zero banana width models. In this paper, detailed comparisons between the calculated ICRF power deposition profiles and experimentally measured quantities will be presented which indicate that significant deviations from the zero banana width models occur even for modest power levels ($P_{rf} \sim 6$ MW) in the TFTR experiments.

EXPERIMENTAL OBSERVATIONS AND ANALYSIS

ICRF heating experiments on TFTR were performed in the deuterium majority/hydrogen minority regime at power levels up to 8.4 MW with $(0-\pi)$ phasing. A plasma current of 1.8 MA was used and the toroidal field was set at about 3.2 T to insure on-axis heating for a source frequency of 47 MHz. Central densities ranged from $3.8-5.5 \times 10^{13} \text{ cm}^{-3}$ with z_{eff} typically about 1.5-1.8 for these discharges. According to spectroscopic measurements, the H/(H+D) ratio at the edge of these plasmas was in the range of 5%-8%, leading to an inferred central hydrogen density of about 6%. At ICRF power lev-

MASTER

RECEIVED

APR 23 1993

OSTI

DISTRIBUTION OF THIS DOCUMENT IS UNLIMITED

els above 3 MW, the sawteeth were either stabilized or significantly lengthened during the RF pulse. The time evolution of the central electron temperature and density for discharges with 3.2 and 8.4 MW are displayed in Fig. 1.

From the magnetics measurements for the total stored energy, W_{tot} , and the diamagnetic stored energy, W_{dia} , the excess perpendicular stored energy, W_{\perp} , in each discharge can be estimated as $W_{\perp} = 3 W_{\text{dia}} - 2 W_{\text{tot}}$. This measurement is compared in Fig. 2 with estimates obtained from an equilibrium energy balance analysis, W_{kin} , and from calculations of the integrated tail stored energy, W_{code} , obtained using the SNAP RF model⁵. Since the ion temperature was not measured directly in these discharges, the ion temperature profile was calculated assuming that $\chi_i = \alpha \chi_e$, with α determined so that the measured and calculated neutron production rates were in agreement. For these discharges, α was typically in the range of 1-2. By subtracting the measured electron stored energy and the inferred ion stored energy components from W_{tot} , the kinetic estimate of the tail stored energy was obtained. Note that W_{\perp} and W_{kin} are consistent to within the experimental accuracy of the data. However, W_{code} is consistently higher than both W_{\perp} and W_{kin} , the discrepancy becoming more pronounced at the higher RF power levels.

Passive charge exchange measurements of the minority hydrogen distribution as a function of energy, obtained using the alpha charge exchange diagnostic, are shown in Fig. 3 for different RF power levels. Estimates for the hydrogen tail temperature for each discharge, obtained from straight line fits to the curves, are compared against the model predictions in Fig. 4. Despite the large discrepancies between the measured and predicted values for the volume-integrated fast ion energy content, as evidenced in Fig. 2, the model predictions for T_{tail} agree reasonably well with the charge exchange measurements.

DISCUSSION

Comparisons between the predicted ICRF power deposition profiles and the measured total fast ion stored energy and effective temperature for the high RF power TFTR experiments lead to the paradoxical conclusion that while the computed fast ion temperatures are in rough agreement with the data, the computed total fast ion stored energy is a factor of 2-3 too high, particularly at the higher RF power levels. A similar disagreement between the computed and measured total stored energy of the fast ion has been noted in the JET experiments and ascribed to finite orbit width effects^{3,4}. According to the JET model³, finite orbit width effects become significant when the radial

width of the fast ion orbit is comparable to the width of the focal spot of the RF power deposition. This condition is satisfied for tail temperatures above a critical value, which for both TFTR and JET is on the order of 0.875-1 MeV. In the TFTR discharges studied here, the tail temperature, as measured and as computed with a zero banana width model, is significantly lower than this critical value in most cases. Furthermore, the finite orbit width model also predicts a significant decrease in the peak tail temperature, a result which is inconsistent with the TFTR data. While the predicted tail temperatures typically exceed the measured temperatures by about 10%, the overall implication is that finite orbit width effects can not account for the discrepancy between the experimental results and the model.

An alternate cause for the differences between the measurements and the model may be the presence of TAE mode activity in these discharges^{1,6}. The relative amplitude of the magnetic perturbations associated with the TAE modes is plotted in Fig. 5, showing a strong increase with applied RF power. The TAE modes excited in these experiments tend to peak off-axis. It is possible that enhanced hot ion loss associated with these modes could lead to a decrease in the fast ion stored energy at radii where the TAE mode peaks. Such an enhanced hot ion loss has been observed in the ⁴He(H) experiments^{1,6}. This could lead to an overall decrease in the volume integrated fast ion stored energy while having a minimal effect on the central tail temperature. Self-consistent transport studies of the power deposition in these discharges will need to be completed before the relative importance of the TAE mode activity and the finite orbit width effects on the fast ions can be quantified.

*Work supported by U.S.D.O.E. Contract # DE-AC02-76-CHO-3073

†Oak Ridge National Laboratory, Oak Ridge TN 37831-8072

#Ioffe Institute, St. Petersburg, Russia

REFERENCES

1. J.R. Wilson, M. Bell, H. Biglari, et al., to be published in Proceedings of the Fourteenth Int. Conf. on Plasma Physics and Controlled Nuclear Fusion Research, September 1992, Wurzburg, Germany, paper IAEA-CN-56/E22.
2. S.J.Zweben, R. Boivin, D.S. Darrow, et al., IBID, paper IAEA -CN-56/A-6-3.
3. G.A. Cottrell and D.F.H. Start, Nuclear Fusion **31**,61 (1991).
4. M.A. Kovanen, W.G.F. Core and T. Hellsten, Nuclear Fusion **32**,787 (1992).
5. D.N. Smithe, C.K. Phillips, G.W. Hammett, and P.L. Colestock, Radio-Frequency Power in Plasmas, AIP Conference Proc. 190, (AIP, N.Y. , 1989) p. 338.
6. J.R. Wilson, K.L. Wong, E. Fredrickson, et al., submitted to Phys. Rev. Lett.

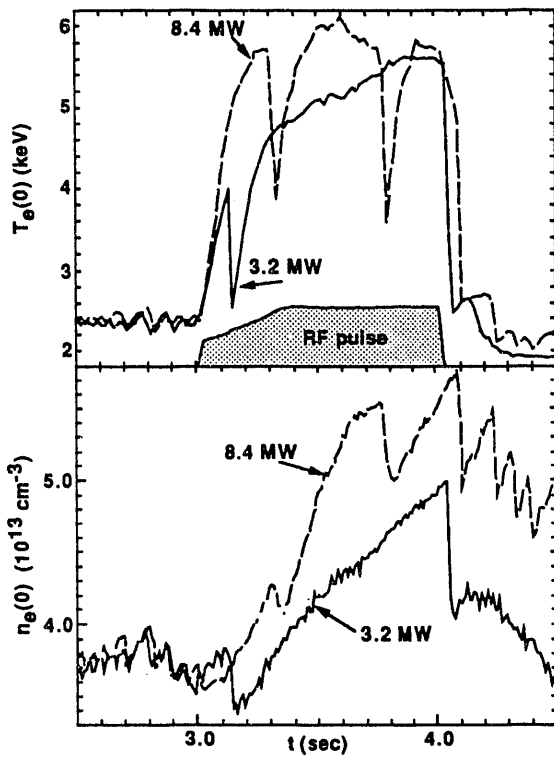


Fig. 1 Time evolution of two sample discharges

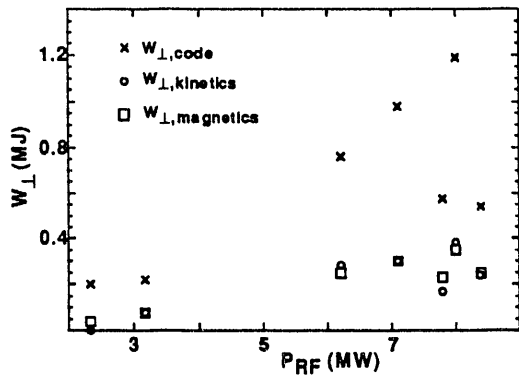


Fig. 2 Comparisons of calculated and measured perpendicular stored energy

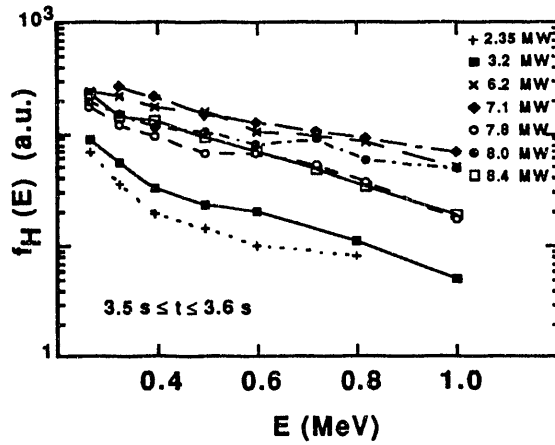


Fig. 3 CX measurements of energetic hydrogen distribution function

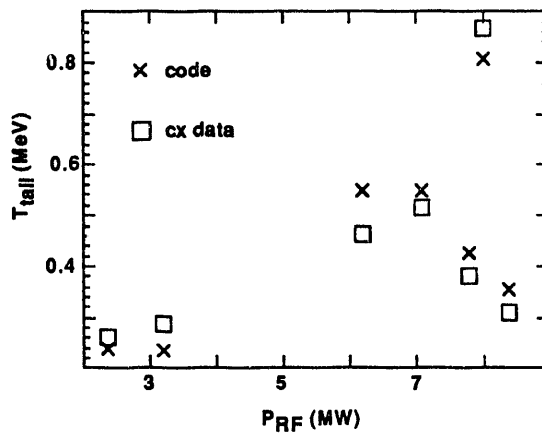


Fig. 4 Comparisons of measured and calculated hydrogen tail temperatures

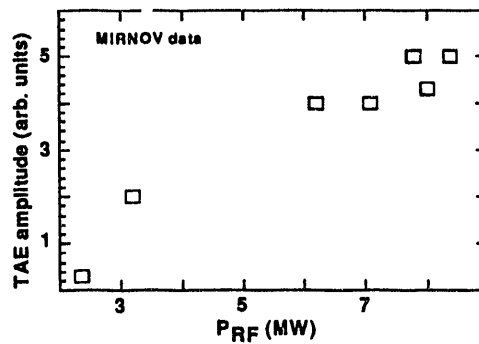


Fig. 5 Amplitude of magnetic perturbation of TAE mode

**DATE
FILMED**

6 / 17 / 93

